

## Transverse instability and riddled basins in a system of two coupled logistic maps

Yu. L. Maistrenko, V. L. Maistrenko, and A. Popovich

*Institute of Mathematics, National Academy of Sciences of Ukraine, 3 Tereshchenkivska street, Kiev 252601, Ukraine*

E. Mosekilde

*Center for Chaos and Turbulence Studies, Department of Physics, Technical University of Denmark, 2800 Lyngby, Denmark*

(Received 19 June 1997)

Riddled basins denote a characteristic type of fractal domain of attraction that can arise when a chaotic motion is restricted to an invariant subspace of total phase space. An example is the synchronized motion of two identical chaotic oscillators. The paper examines the conditions for the appearance of such basins for a system of two symmetrically coupled logistic maps. We determine the regions in parameter plane where the transverse Lyapunov exponent is negative. The bifurcation curves for the transverse destabilization of low-periodic orbits embedded in the chaotic attractor are obtained, and we follow the changes in the attractor and its basin of attraction when scanning across the riddling and blowout bifurcations. It is shown that the appearance of transversely unstable orbits does not necessarily lead to an observable basin riddling, and that the loss of weak stability (when the transverse Lyapunov exponent becomes positive) does not necessarily destroy the basin of attraction. Instead, the symmetry of the synchronized state may break, and the attractor may spread into two-dimensional phase space. [S1063-651X(98)05303-3]

PACS number(s): 05.45.+b

### I. INTRODUCTION

A problem that arises in many fields of science is related to the behavior of a group of interacting entities or functional units, each of which displays deterministic chaos or other forms of complex nonlinear dynamic behavior. Fujisaka and Yamada [1] showed how two identical chaotic systems under variation of the coupling strength can attain a state of chaotic synchronization in which the motion of the coupled system takes place on an invariant subspace of total phase space. For two coupled identical one-dimensional maps, for instance, the synchronized chaotic motion is one dimensional, and occurs along the main diagonal in phase plane. The transverse Lyapunov exponent  $\lambda_{\perp}$  provides a measure of the average stability of the chaotic attractor perpendicularly to this direction.

Chaotic synchronization was subsequently studied by numerous investigators [2–5], and a variety of applications for chaos suppression, for monitoring of dynamical systems, and for different communication purposes have been suggested. An important question concerns the form of the basin of attraction for the synchronized state and the bifurcations through which this basin, or the attractor itself, undergoes qualitative changes. Particularly interesting are the phenomena of riddled basins of attraction [6–8] and on-off intermittency [9], that can be observed on either side of the so-called blowout bifurcation [7], where the transverse Lyapunov exponent  $\lambda_{\perp}$  changes sign.

On-off intermittency is an extreme form of intermittent bursting [10,11] that occurs in the presence of a small positive value of  $\lambda_{\perp}$  [9]. In this case the chaotic set on the invariant subspace is no longer transversely attracting on the average. However, immediately above the bifurcation, a trajectory may spend a very long time in the neighborhood of the invariant subspace. From time to time, the repulsive character of the chaotic set manifests itself, and the trajectory

exhibits a burst in which it moves far away from the invariant subspace, to be reinjected again into the proximity of this subspace. Besides a reinjection mechanism, the occurrence of on-off intermittency hinges on the fact that the positive value of the transverse Lyapunov exponent applies over long periods of time. For shorter time intervals, the net contribution to  $\lambda_{\perp}$  may be negative, and the trajectory is attracted to the chaotic set [9].

If there is no reinjection mechanism, a trajectory started near the invariant subspace may exhibit a superpersistent chaotic transient in which the behavior initially resembles the chaotic motion before the blowout bifurcation. Eventually, however, almost all trajectories will move away from this region and approach some other attractor (or go to infinity). Alternatively, the blowout bifurcation can lead to an attractor which is confined by nonlinear mechanisms to a region of phase space (the absorbing area) situated inside the original basin of attraction, and this basin remains practically unchanged in the bifurcation. Variation of a parameter that causes the attractor to grow (or the basin to shrink) may then produce a crisis in which the attractor abruptly disappears as it makes contact with the basin boundary [12].

Riddled basins of attraction may be observed on the other side of the blowout bifurcation, where the transverse Lyapunov exponent is numerically small and negative [6,7,13–15]. Even though the chaotic set is now attractive on the average, particular orbits (usually of low periodicity) embedded in the chaotic attractor may be transversely unstable. In this case we talk about weak attraction or attraction in the Milnor sense [16]. The chaotic set in the invariant subspace then attracts a set of points of positive Lebesgue measure in phase space. However, arbitrarily close to any such point one may find a positive Lebesgue measure set of points that are repelled by the chaotic attractor.

The emergence of riddled basins of attraction occurs through a so-called riddling bifurcation (sometimes referred

to as a bubbling transition [13]), in which an orbit embedded in the synchronized chaotic attractor loses its transverse stability. This phenomenon was recently been described in detail by Lai *et al.* [17]. They suggested that the riddling bifurcation takes place as two repellers located symmetrically on either side of the invariant subspace approach the chaotic attractor and collide with a saddle embedded in this attractor (a so-called saddle-repeller pitchfork bifurcation). Alternatively, a point cycle embedded in the synchronized state may lose its transverse stability through a period-doubling bifurcation. This situation, which appears to have been given less attention, plays a significant role in the present analysis. In both cases, i.e., for the pitchfork as well as for the period-doubling bifurcation, the transition may be subcritical or supercritical depending on the sign of a certain quantifier. After a supercritical bifurcation, the transversely destabilized orbit will be surrounded by saddle points with unstable manifolds along the invariant subspace of the synchronized state. This leads to attractor bubbling and to the phenomenon of local riddling [13,15]. In this case, the trajectories cannot escape an area around the synchronized state until one or two additional (global) bifurcations have occurred [18].

The riddling bifurcation causes tongues of finite width to open up along the transversely unstable directions from each point on the repelling orbit [17], and in these tongues trajectories move away from the chaotic attractor. Similar tongues open up from each preimage of the points on the repelling orbit, and since the points of this orbit and their preimages are dense in the invariant subspace, an infinite number of tongues emerge, creating the characteristic riddled structure in which the basin of attraction locally becomes a fat fractal.

Maistrenko and Kapitaniak [19] recently studied chaotic synchronization and the formation of riddled basins of attraction for a system of two coupled piecewise linear maps. They related the various phenomena to the different types of instability for the chaotic set in the invariant subspace. By virtue of the simplicity of the map, they succeeded in deriving the corresponding stability conditions. Also investigating coupled piecewise linear maps, Pikovsky and Grassberger [20] discovered that even when the coupled system exhibits a stable synchronized behavior as indicated by the negative value of the transversal Lyapunov exponent, the basin of attraction may have full measure but be densely filled with periodic orbits. Hence the synchronized attractor is surrounded by a strange invariant set which is dense in an area around the attractor, and the synchronized state is not asymptotically stable. Pikovsky and Grassberger [20] also observed a bifurcation in which a synchronized one-dimensional attractor explodes into a two-dimensional attractor that contains the strange invariant set. Gardini *et al.* [21] recently investigated a one-parameter family of twisted, logistic maps. Of special interest in the present context is their analysis of the role of contact bifurcations (boundary crises) in which the boundary of the absorbing area for a chaotic set makes contact with the basin boundary. This type of global bifurcations are involved in the transition from local to global riddling [18].

The purpose of the present paper is to study the emergence of riddled basins in a two-dimensional map  $F = F_{a,\epsilon}: R^2 \rightarrow R^2$  of the form

$$F: \begin{cases} x \\ y \end{cases} \rightarrow \begin{cases} f_a(x) + \epsilon(y-x) \\ f_a(y) + \epsilon(x-y) \end{cases}, \tag{1}$$

where  $f_a$  is the one-dimensional logistic map,

$$f_a: x \rightarrow ax(1-x), \quad x \in R^1, \quad a \in [0,4], \tag{2}$$

and  $\epsilon \in R^1$  is the coupling parameter. We determine the regions of weak stability in the  $a\epsilon$  plane for the synchronized chaotic attractor, and calculate the transverse Lyapunov exponent  $\lambda_{\perp}$  as a function of  $\epsilon$  for characteristic values of  $a$  where the individual map shows a homoclinic bifurcation (chaotic band merging). These are the parameter values at which  $f_a(x)$  is known to display a chaotic attractor with an absolutely continuous invariant measure.

The formation of riddled basins of attraction is discussed, and the bifurcation curves for the transverse destabilization of low-periodic orbits embedded in the chaotic attractor are determined. For one-band, two-band, and four-band chaotic attractors we follow the changes in the attractor and its basin of attraction that take place under passage of the riddling and the blowout bifurcations. It is shown that the loss of weak stability does not necessarily affect the basin of attraction. Instead, the chaotic attractor may spontaneously break the symmetry and spread into two-dimensional phase space. It is also shown that the emergence of transversely unstable trajectories, while being a necessary condition for basin riddling, is not sufficient for global riddling to occur. Finally, we illustrate the phenomenon of intermingled basins of attraction [6] for a situation where the system has two coexisting four-band attractors, each displaying a riddled basin structure.

## II. WEAK STABILITY OF THE SYNCHRONIZED CHAOTIC STATE

The metric and topological properties of the logistic map are well studied [22,23]. It is known, for instance, that for any  $a \in [0,4]$ :  $f_a$  has no more than a single attracting cycle. The parameter set  $\mathcal{L} = \{a \in [0,4]: f_a \text{ has an attracting cycle}\}$  is open and everywhere dense [24]. At the same time, the parameter set  $\mathcal{K} = \{a \in [0,4]: f_a \text{ has an absolutely continuous invariant measure}\}$  is nowhere dense (i.e., it has a Cantor-like structure), and the measure  $\mu(\mathcal{K}) > 0$  [25].

Figure 1 shows part of the bifurcation diagram for the logistic map with the well-known period-doubling cascade of attracting cycles  $\gamma_{2^n}$ . Increasing the parameter  $a$  beyond the accumulation point  $a^* \cong 3.569$  for this cascade, a reverse cascade of homoclinic bifurcations of the cycles  $\gamma_{2^n}$  takes place at the parameter values  $a_n$ . In  $a_0$ , for instance, the unstable fixed point  $x_0 = 1 - 1/a$  undergoes its first homoclinic bifurcation.

The bifurcation points  $a_n$  can easily be determined numerically ( $a_0$  can also be calculated explicitly). The first four are given by

$$\begin{aligned} a_0 &= 3.678\ 573\ 510\ 428\ 32 \dots, \\ a_1 &= 3.592\ 572\ 184\ 106\ 97 \dots, \\ a_2 &= 3.574\ 804\ 938\ 759\ 20 \dots, \\ a_3 &= 3.570\ 985\ 940\ 341\ 61 \dots \end{aligned}$$

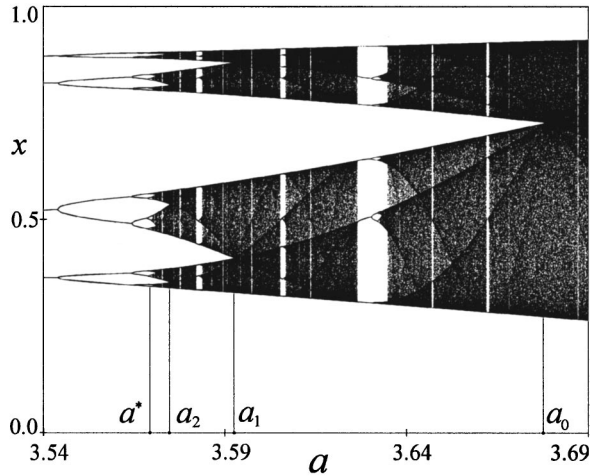


FIG. 1. Bifurcation diagram for the individual map  $f_a: x \rightarrow ax(1-x)$  for  $3.54 \leq a \leq 3.69$ . At each of the homoclinic bifurcation points  $a_n$ , the map has an absolutely continuous invariant measure.

At  $a = a_0$ ,  $f_a$  has an attracting interval  $\Gamma_0 = [f_a(a_0/4); (a_0/4)]$  consisting of two subintervals  $\Gamma_0 = [f_a(a_0/4); x_0] \cup [x_0; (a_0/4)]$  which are permuted one into the other under the action of  $f_a$ . Moreover,  $f_a$  has an absolutely continuous invariant measure in  $\Gamma_0$ . Hence the map is chaotic. Similarly, for  $a = a_n$ ,  $f_a$  has an attracting cycle  $\Gamma_{2^n}$  of  $2^n$  intervals consisting of  $2^{n+1}$  subintervals that are pairwise permuted under the action of  $f_a^{2^n}$ . Moreover, having an absolutely continuous invariant measure,  $f_a$  is chaotic in  $\Gamma_{2^n}$ .

The main diagonal  $\{x=y\}$  is a one-dimensional invariant manifold of the two-dimensional map  $F$ . This implies that a point on the diagonal will be mapped into another point on this line, or, in other words,  $F(\{x=y\}) \subset \{x=y\}$ . The existence of such a one-dimensional invariant manifold is clearly a consequence of the restrictions imposed by the symmetric coupling of two identical one-dimensional maps. Any small mismatch between the maps leads, in general, to the disappearance of the one-dimensional manifold, with the result that the dynamics becomes two dimensional.

By subtracting the two one-dimensional maps in Eq. (1), one finds a transversal line  $\{x+y=1-2\varepsilon/a\}$  that also maps onto the main diagonal under the action of  $F$  [26]. This line is the preimage of the main diagonal, and part of the line (which maps into the attractive interval on the main diagonal) will belong to the basin of attraction for stable solutions on the diagonal. By adding the two one-dimensional maps in Eq. (1), one can show that the preimage of the transversal line is a circle centered in  $(x,y) = (1/2, 1/2)$  and with radius  $(a^2 - 2a + 4\varepsilon)^{1/2}/a\sqrt{2}$ .

For any point on the main diagonal,  $F_{a,\varepsilon}$  has an eigendirection  $\bar{u}_1 = (1,1)$  along the diagonal, and an eigendirection  $\bar{u}_2 = (1,-1)$  perpendicular to it. The corresponding eigenvalues are

$$v_1 = f'_a(x) = a(1-2x) \quad (3)$$

and

$$v_2 = f'_a(x) - 2\varepsilon = a(1-2x) - 2\varepsilon. \quad (4)$$

Along the diagonal, the coupling vanishes, and the dynamics coincides with that of the one-dimensional map  $f_a(x)$ . Let  $I \subset \mathbb{R}^1$  be a chaotic attractor for  $f_a(x)$ , then  $A = \{x=y \in I\}$  will be a one-dimensional invariant chaotic set for the coupled map system.  $A$  attracts points from its one-dimensional neighborhood along the diagonal. Does it also attract points from its two-dimensional neighborhood  $U_\delta(A)$ ? In other words, is  $A$  an attractor in the plane? The answer to this question clearly depends on the values of the transverse eigenvalues at all the different points of  $A$ .

As a first approach to addressing this problem we may evaluate the transverse Lyapunov exponent

$$\lambda_\perp = \lim_{N \rightarrow \infty} \frac{1}{N} \sum_{n=1}^N \ln |f'_a(x_n) - 2\varepsilon|, \quad (5)$$

where  $\{x_n = f_a^n(x)_{n=1}^\infty\}$  is a typical itinerary on  $A$ . If the set  $A$  has an absolutely continuous invariant measure, e.g., for the above mentioned parameters values  $a_n$ , the value of  $\lambda_\perp$  will be the same for almost all trajectories on  $A$ . If  $\lambda_\perp$  is negative, we expect that  $A$  is attracting on the average in a two-dimensional neighborhood. This type of stability is referred to as weak stability or stability in the Milnor sense [16].

Indeed, as shown by Alexander and co-workers [6], in the case that  $A$  is a finite union of intervals and the invariant measure of  $f_a$  on  $A$  is absolutely continuous, the condition  $\lambda_\perp < 0$  guarantees that  $A$  attracts a positive Lebesgue measure set of points from any two-dimensional neighborhood  $U_\delta(A)$ . Moreover, weak stability in the Milnor sense implies that the measure of points attracted to  $A$  approach the whole measure of  $U_\delta(A)$  as the width of the neighborhood  $\delta \rightarrow 0$ , i.e.,

$$\lim_{\delta \rightarrow 0} \frac{\mu(B(A) \cap U_\delta(A))}{\mu U_\delta(A)} = 1. \quad (6)$$

Here  $B(A)$  denotes the basin of attraction of  $A$ , i.e., the set of points  $(x,y) \in \mathbb{R}^2$  for which the  $\omega$  limit is contained in  $A$ . The transition in which  $\lambda_\perp$  changes sign is referred to as a blowout bifurcation [8].

Figure 2 shows the regions of parameter space in which  $\lambda_\perp < 0$ , so that the synchronized attractor is (at least) weakly stable. The figure was obtained by performing 1000 scans of  $\lambda_\perp(\varepsilon)$  for different values of  $a$  with a corresponding resolution on the  $\varepsilon$  axis. The stability regions clearly reflect the complexity of the bifurcation structure. In particular, we notice the irregular variation with  $a$  in the chaotic regime. For values of  $a$  below the accumulation point  $a^* \approx 3.569$ , the individual map displays an attracting cycle, and the synchronized behavior is also periodic. In this case there is no distinction between weak and asymptotic (or strong) stability.

In each of the periodic windows in the region  $a > a^*$ , the distinction between weak and strong stability likewise disappears. Moreover, for an  $N$ -periodic synchronous state  $\gamma_N = \{x_1, x_2, \dots, x_N\}$ , the criterion for transverse stability

$$\prod_{n=1}^N |f'_a(x_n) - 2\varepsilon| < 1, \quad (7)$$

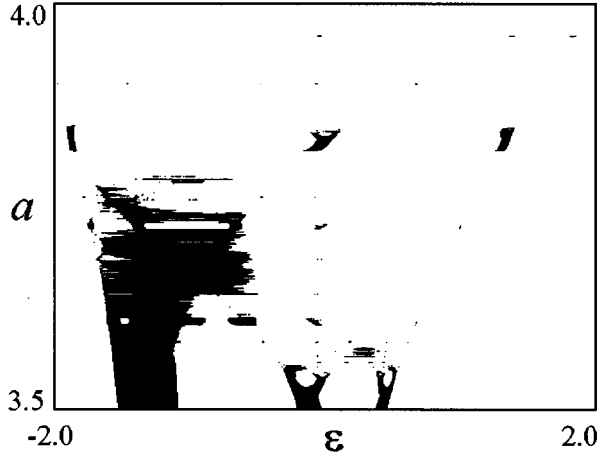


FIG. 2. Region in parameter plane in which the transversal Lyapunov exponent  $\lambda_{\perp} < 0$ .

is satisfied if and only if the coupling parameter  $\varepsilon$  belongs to the union of  $N$  (possibly overlapping) intervals, each including one point from  $\gamma_N$ . Some of these intervals correspond to positive values for  $\varepsilon$ , and some of them correspond to  $\varepsilon < 0$ .

The stability intervals are clearly seen in Fig. 2. We notice, for instance, the stability regions for the period-6 solution around  $a = 3.63$ , for the period-5 solution around  $a = 3.74$ , and for the period-3 solution in the interval around  $a = 3.84$ . For each of these windows we also observe the signature of the period-doubling cascade in which they end. In a similar manner, the two-band chaotic attractor existing for  $a = a_1$ , may give rise to a two  $\varepsilon$  intervals with  $\lambda_{\perp} < 0$ , and the four-band chaotic attractor existing for  $a = a_2$  may have four (partly overlapping) intervals for  $\varepsilon$  with weak stability.

**III. FORMATION OF RIDDLED BASINS OF ATTRACTION**

The condition  $\lambda_{\perp} < 0$  guarantees that almost all trajectories on  $A$  are transversally attracting. However, there can still be an infinite set of trajectories in the neighborhood of  $A$  that are repelled from it. As we shall see, this situation is quite generic for our system of coupled logistic maps. To obtain an attractor in the usual (topological) sense, we must ascertain that all trajectories on  $A$  are transversally attracting.

Consider, for example, the fixed point  $P(x_0, x_0)$ . Inserting  $x_0 = 1 - 1/a$  into Eq. (4) and requiring that the magnitude of  $\nu_2$  be less than 1, we find a coupling interval [18]

$$-\frac{a-1}{2} < \varepsilon < -\frac{a-3}{2},$$

in which the fixed point is transversally stable. If  $a > 3$  and  $\varepsilon$  falls outside this interval, both  $\nu_1$  and  $\nu_2$  will be numerically larger than 1, and  $P$  will be a repelling node.

Under the action of  $F_{a,\varepsilon}$ , a trajectory starting close to the fixed point moves away from it along an integral curve. Under sufficiently general conditions ( $\nu_1 \neq \nu_2$ ), these integral curves take the asymptotic form

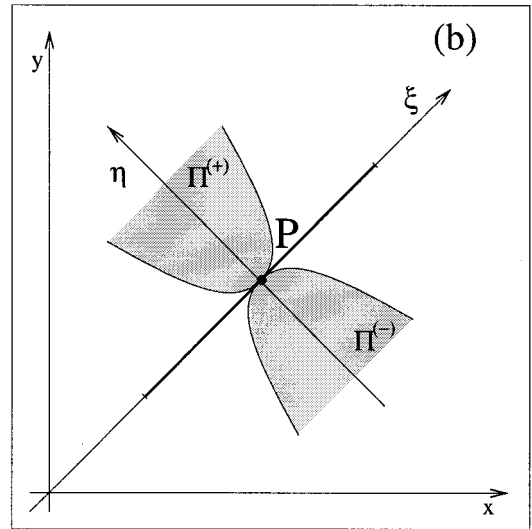
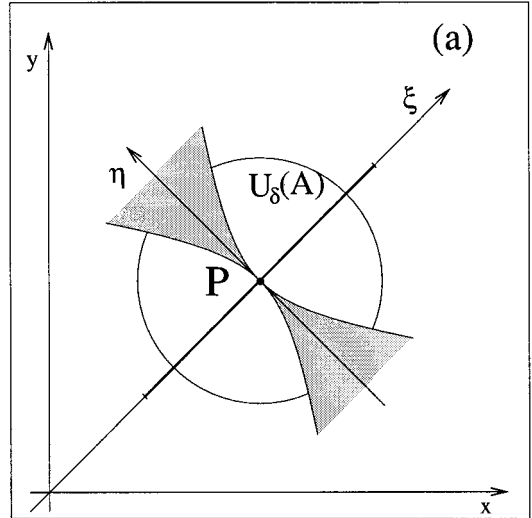


FIG. 3. The two generic forms for the repelling tongues that develop from each point on a transversally unstable periodic cycle.

$$|\eta| = C|\xi|^{|\ln|\nu_2|/|\ln|\nu_1|} + O(|\xi|), \tag{8}$$

where  $\xi = x + y - 2x_0$  and  $\eta = -x + y$  are new coordinates defined along and perpendicular to the diagonal, respectively.  $C$  is an arbitrary constant, depending on the initial conditions. Expression (8) is obtained as the solution to the linearized map  $DF$  around the fixed point. It follows from Eq. (8) that the integral curves are tangent to the  $\eta$  axis for  $|\nu_2| < |\nu_1|$  and tangent to the  $\xi$  axis for  $|\nu_2| > |\nu_1|$ . These two situations are illustrated in Fig. 3.

Now consider a neighborhood  $U_{\delta}(P)$  of the fixed point, and assume that  $\delta$  is small enough for the linear approximation (8) to apply. Then, except for the fixed point itself, all points belonging to the unstable manifold  $\xi = 0$  will leave  $U_{\delta}$  under the action of  $DF$ . Moreover, all points  $(\xi, \eta)$  in the region

$$\Pi_0 = \{(\xi, \eta) : |\eta| \leq C|\xi|^{|\ln|\nu_2|/|\ln|\nu_1|}\} \quad (C \text{ fixed}) \tag{9}$$

will also leave  $U_{\delta}$  under the action of  $DF$ . If  $|\nu_2| < |\nu_1|$ , the region  $\Pi_0$  is the unity of two tongues  $\Pi_0^{(+)}$  and  $\Pi_0^{(-)}$ , approaching the fixed point from either side in a cusp [Fig.

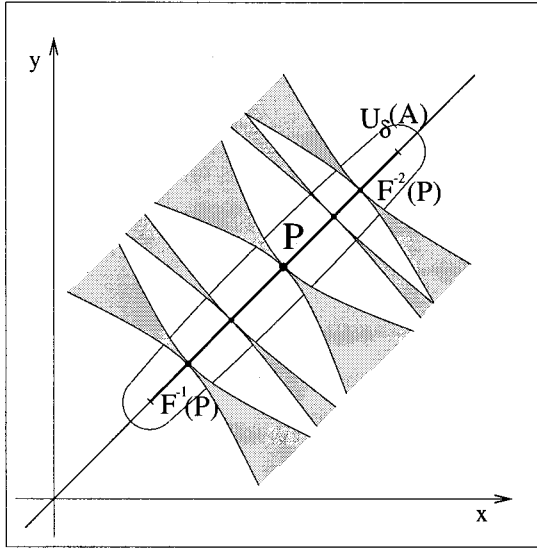


FIG. 4. The riddling bifurcation produces a dense set of repelling tongues.

3(a)]. If  $|\nu_2| > |\nu_1|$ , on the other hand, the tongues  $\Pi_0^{(+)}$  and  $\Pi_0^{(-)}$  are tangent to the diagonal in the fixed point. Both of these situations can arise in our system of two coupled logistic maps.

We can now conclude the following with respect to  $F$ : In a sufficiently small neighborhood  $U_\delta(P)$ , the integral curves of the map  $F$  form invariant regions consisting of a pair of tongues  $\Pi^{(+)}$  and  $\Pi^{(-)}$ . For any fixed  $C$  these tongues can be obtained through smooth perturbations of the tongues  $\Pi_0^{(+)}$  and  $\Pi_0^{(-)}$  obtained in the linear case, and hence have similar topological properties: They lie on either side of the main diagonal  $\{x=y\}$  and touch it in the fixed point. If  $|\nu_2| > |\nu_1|$ ,  $\Pi^{(+)}$  and  $\Pi^{(-)}$  are tangent to the diagonal in  $P$ .

Let us now suppose that the fixed point  $P(x_0, x_0)$  belongs to the chaotic attractor  $A$  on the main diagonal, and that  $A$  has an absolutely continuous invariant measure. The fixed point  $P$  will then have infinitely many preimages, and the set of these preimages will be dense in  $A$ . It can also be expected that the set  $U_\delta^u$  of preimages of the tongues  $\Pi^{(+)}$  and  $\Pi^{(-)}$  will be dense in some neighborhood of  $A$  (except in some half-neighborhoods of end points for the intervals that span the attractor). This situation is illustrated in Fig. 4.

$U_\delta^u$  is the locally repelling set of the attractor  $A$ , and each point from  $U_\delta^u \setminus A$  leaves the neighborhood  $U_\delta(A)$  in a finite number of iterations. It is important to note that this repelling property has a local character. Our analysis says nothing about the fate of the trajectories once they have left the neighborhood  $U_\delta$ . This depends on the global dynamics of  $F$ , and two different scenarios may occur.

#### Scenario 1

Having left the locally repelling region  $U_\delta^u(A)$ , the trajectories wander around in phase space. However, they are restricted by nonlinear mechanisms to move within an absorbing area [21] that lies strictly inside the basin of attraction. The trajectories can never approach an attractor outside the absorbing area, and global riddling of the basin of attraction cannot occur. Sooner or later most of the trajectories will return to  $U_\delta(A)$ . Some of them may again be mapped into

$U_\delta^u(A)$  and, hence, again leave the neighborhood of  $A$  in a finite number of iterations. This type of dynamics gives rise to the characteristic temporal bursting of on-off intermittency. As long as the transverse Lyapunov exponent is positive, the bursts will never stop, and in reality we have an attractor in two-dimensional phase space with a more or less pronounced maximum of its invariant density in the neighborhood of the original one-dimensional attractor. As  $\lambda_\perp$  becomes negative, the bursts tend to stop. However, this transition may not be very sharp, and one may still see some bursting even for negative values of  $\lambda_\perp$  (attractor bubbling). It should be noted that more than one attractor may exist inside the absorbing area. If this is the case, one may observe global riddling of the basins of attraction for these coexisting states.

#### Scenario 2

If the nonlinear mechanisms are too weak to restrict the motion to an absorbing area inside the basin of attraction for the synchronized state, the alternative is that almost all points leaving  $U_\delta^u(A)$  go to another attractor. This could be an attracting point cycle, a chaotic attractor or infinity. On the other hand, provided that  $\lambda_\perp < 0$ , the measure of the complementary set  $U_\delta^s \subset U_\delta \setminus U_\delta^u$  of points that are attracted to  $A$  and never leave  $U_\delta$  approaches the measure of  $U_\delta$  for  $\delta \rightarrow 0$  [6]. This result applies at least as long as  $A$  is a one-dimensional attractor consisting of a finite number of intervals and with an absolutely continuous invariant measure. Under these conditions we expect the basin of attraction to attain a globally riddled structure with holes that belong to the basin of another attractor. Mathematically expressed, this implies that, for any  $\delta > 0$ , (1) the complementary set  $U_\delta(A) \setminus \mathcal{B}(A)$  is everywhere dense in  $U_\delta$ , and (2)  $0 < \mu[\mathcal{B}(A) \cap U_\delta(A)] < \mu[U_\delta(A)]$ .

In contrast to this, the case of strong (or absolute) stability is characterized by the existence of a  $\delta > 0$  such that  $\mathcal{B}(A) \supset U_\delta = U_\delta^s$ . This requires that all trajectories on  $A$  are transversely stable.

In order to determine the boundaries in parameter space for the regions of absolute stability for the synchronized chaotic attractor, we may start by considering the transverse stability of the various point cycles embedded in this attractor. We have already seen that the conditions for transverse stability for the fixed point are  $-(a-1)/2 < \varepsilon < -(a-3)/2$ . The slanting line denoted ‘‘fixed point’’ in the middle of the stability diagram of Fig. 5 represents the lower edge of this zone. The upper end falls outside the range of coupling strengths considered in the figure. Hence, the fixed point is transversely stable to the right of the period-1 line. Destabilization of the fixed point happens in a pitchfork bifurcation.

The stability intervals for a point cycle of period  $N$  are formally given by Eq. (7). The period-2 cycle arises at  $a = 3$ , and hereafter alternates between the points

$$x_{1,2} = y_{1,2} = \frac{a+1 \pm \sqrt{(a+1)(a-3)}}{2a}. \quad (10)$$

Evaluating the conditions for transverse stability for this cycle gives two intervals for  $\varepsilon$  of which the interval to the left of  $\varepsilon = -1/2$  is given by

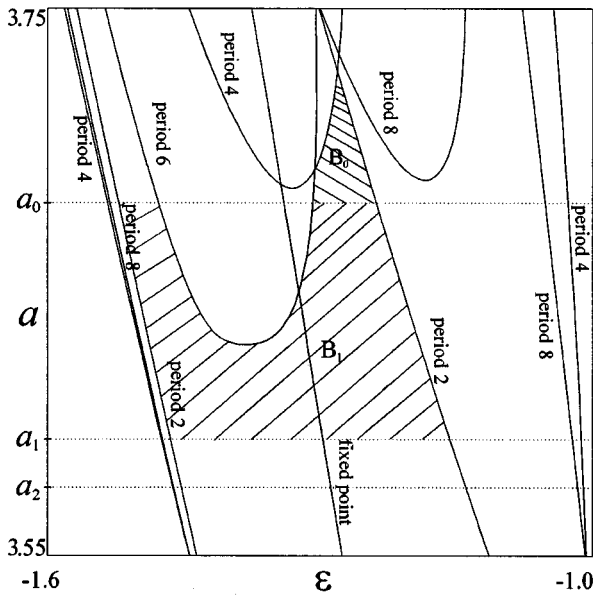


FIG. 5. Bifurcation curves for the transverse destabilization of various low-periodic cycles embedded in the synchronized chaotic attractor.

$$-\frac{1}{2}[1 + \sqrt{(a+1)(a-3)+1}] < \varepsilon < -\frac{1}{2}[1 + \sqrt{(a+1)(a-3)-1}]. \quad (11)$$

The borderlines of this interval are represented by the two curves denoted “period 2” in Fig. 5. The period-2 cycle is transversely stable between these curves. To the right the destabilization happens through a period-doubling bifurcation and to the left through a pitchfork bifurcation.

Similarly, the curves denoted “period 4,” “period 6,” and “period 8” bound the regions of transverse stability for these cycles. The minimum of the curve for the period-6 cycle falls close to  $a = 3.626$ , where this cycle first arises. With the values of  $a$  considered in the figure, the period-3 cycle has not yet appeared in the individual map. Hence synchronized behavior with this periodicity cannot occur, and the figure delineates the regions of transverse stability for the most important cycles of period less than or equal to  $N=8$ . There are reasons to believe that transverse destabilization of cycles of higher periodicity generally does not play a major role, and this is strongly supported by our numerical calculations. From the information in Fig. 5 we can therefore determine the regions of absolute stability for the synchronized chaotic attractor in each of the intervals  $a_1 \leq a < a_0$  and  $a_0 \leq a$ .

On both sides these regions are bounded by the transverse destabilization of the period-2 cycle which occurs before destabilization of the period-8 and period-4 cycles. For higher values of  $a$ , destabilization of the period-6 cycle limits the region of absolute stability for the synchronized chaotic attractor, and there is also a region in parameter space where destabilization of the period-4 cycle is the first to take place. Below the homoclinic bifurcation point  $a_0$ , destabilization of the fixed point has no significance because the two-band chaotic attractor existing in this range does not contain the

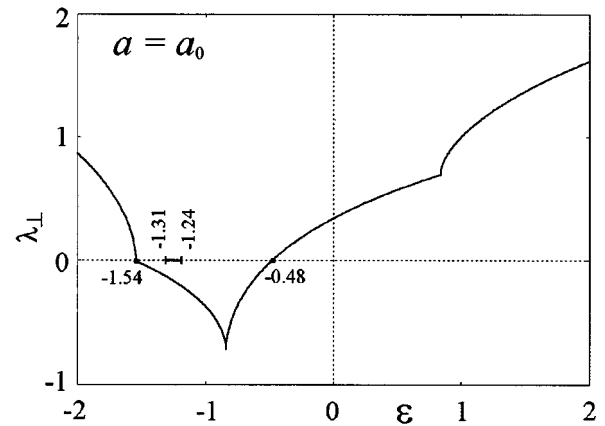


FIG. 6. Variation of the transverse Lyapunov exponent  $\lambda_{\perp}$  with the coupling parameter  $\varepsilon$  for  $a = a_0$ . The synchronized chaotic attractor is absolutely stable for (approximately)  $-1.31 < \varepsilon < -1.24$ .

fixed point. For  $a \geq a_0$ , however, the synchronized chaotic state is no longer asymptotically stable to the left of the period-1 curve.

#### IV. NUMERICAL RESULTS

Figure 6 shows a scan of the transverse Lyapunov exponent  $\lambda_{\perp}$  as a function of the coupling parameter for  $a = a_0$ . For this value of  $a$ , the individual map exhibits a one-band chaotic attractor consisting of two subintervals  $I_1^{(1)}$  and  $I_1^{(2)}$  at the moment when they merge. The points  $\varepsilon \cong -1.544$  and  $\varepsilon \cong -0.478$  where  $\lambda_{\perp}$  changes sign are the blowout bifurcation points. Between these points, the synchronized chaotic state is at least weakly stable. On either side of the points we have a so-called chaotic saddle [13,27]. Also indicated in Fig. 6 is the interval from  $\varepsilon \cong -1.31$  to  $\varepsilon \cong -1.24$  in which the chaotic attractor is absolutely stable.

Figures 7(a)–7(e) portray the basins of attraction for the synchronized chaotic state  $A_0$  at various values of  $\varepsilon$ . In each of these figures initial conditions leading to the chaotic attractor are plotted as grey points, and initial conditions leading to another attractor (or infinity) are left blank.

Figure 7(a) shows the basin of attraction for  $\varepsilon = -1.4$ , i.e., a little to the left of the region of absolute stability. In this region the synchronized period-6 cycle is transversally unstable, and the figure reveals the characteristic appearance of a globally riddled basin with a dense set of tongues with points that are repelled from the attractor emanating from the period-6 cycle and its preimages. As previously noted, the basin of attraction includes a section of a transversal line that maps into the attracting interval of the main diagonal, as well as sections of the circle that is the preimage of the transversal line. From each of these structures we have a similar dense set of repelling tongues, contributing all together to the complexity of the basin.

Figure 7(b) shows the basin of attraction for a coupling parameter immediately to the right of the region of strong stability ( $\varepsilon = -1.2$ ). Here the in-phase period-2 cycle is transversely unstable. However, while the basin has a fractal boundary, there are no tongues in it belonging to the basin of another attractor. This is characteristic of a locally riddled basin of attraction where trajectories repelled from the syn-

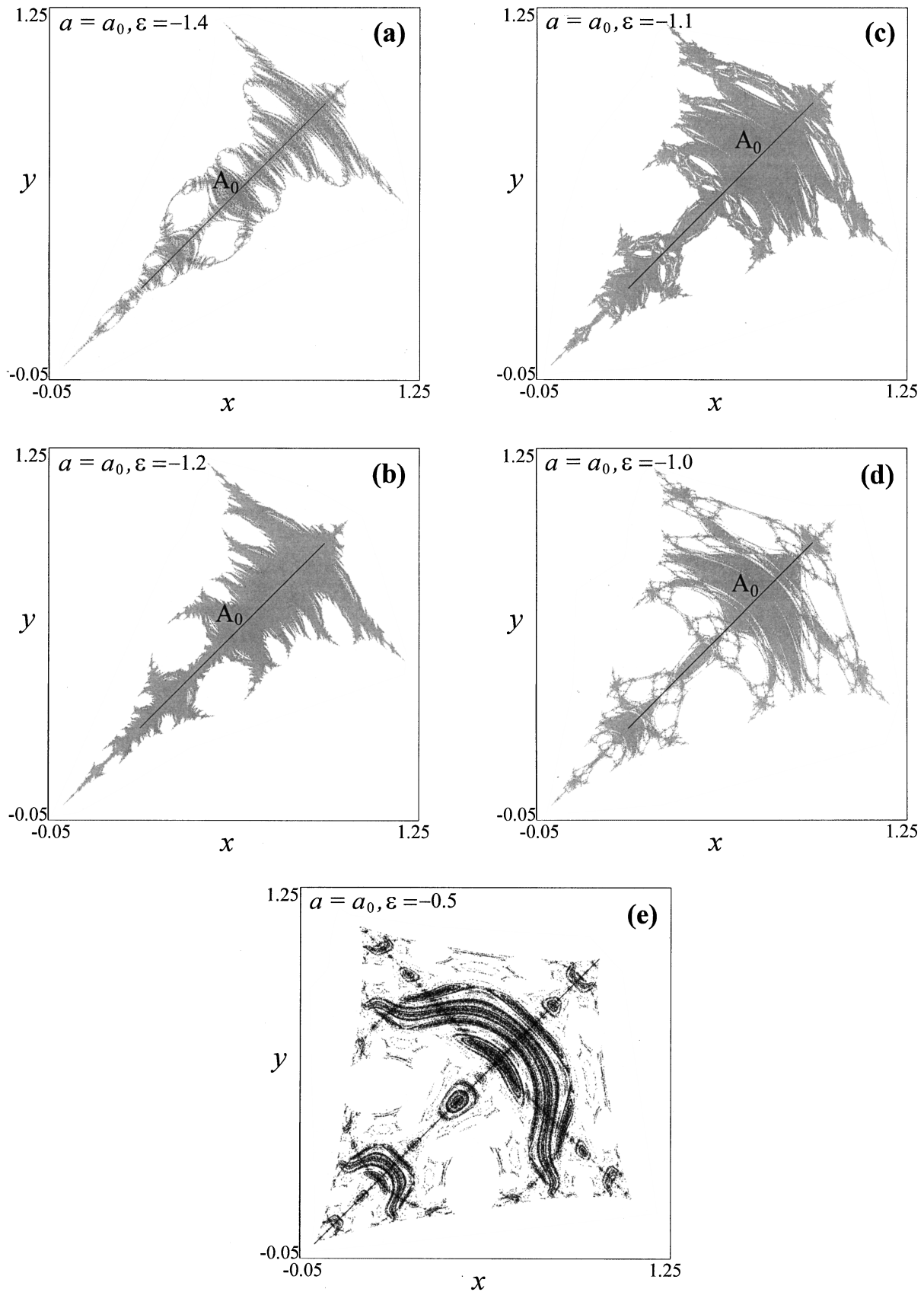


FIG. 7. Basins of attraction for the one-band chaotic attractor  $A_0$  with different values of the coupling constant for  $a = a_0$ : (a) global riddling for  $\varepsilon = -1.4$ , (b) local riddling for  $\varepsilon = -1.2$ , (c) global riddling for  $\varepsilon = -1.1$ , (d) global riddling for  $\varepsilon = -1.0$ , and (e) global riddling close to the blowout bifurcation for  $\varepsilon = -0.5$ . The basin of attraction is plotted grey.

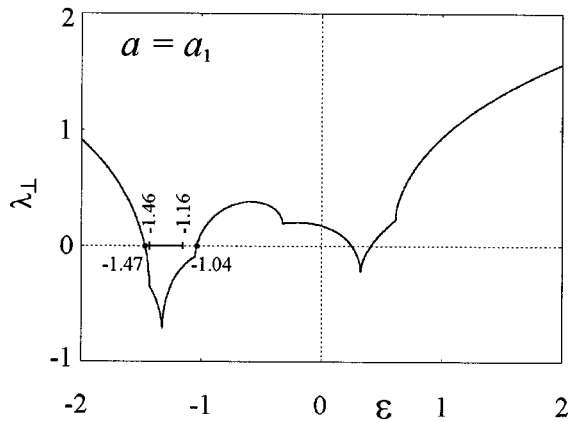


FIG. 8. Variation of the transverse Lyapunov exponent  $\lambda_{\perp}$  with the coupling parameter  $\varepsilon$  for  $a = a_1$ . Here we have two intervals of weak stability. The synchronized attractor is absolutely stable for (approximately)  $-1.46 < \varepsilon < -1.16$ .

chronized chaotic state never reach the basin boundary, and sooner or later return to the neighborhood of the attractor. In this case the synchronized state may be referred to as a Milnor attractor, i.e., it attracts all points from its neighborhood except a set of zero measure.

As  $\varepsilon$  is further increased, a transition occurs in which trajectories repelled from the main diagonal start to make contact with the basin boundary. As illustrated in Fig. 7(c), we then recover the globally riddled structure. Here  $\varepsilon = -1.1$ , and the synchronized state is a weak attractor in the Milnor sense, i.e., there is a finite measure of points in its neighborhood that are repelled from it.

For  $\varepsilon = -1.0$  [Fig. 7(d)], a new structure in the basin of attraction becomes manifest. Here we observe two lines parallel to the main axes and crossing the diagonal at a period-2 point. Each of these lines are invariant with respect to the second iterate of  $F_{a,\varepsilon}$ . A similar set of curves are found to cross the diagonal at the other point of the in-phase period-2 orbit. Finally, in Fig. 7(e),  $\varepsilon \cong -0.5$ , and we are close to the blowout bifurcation at  $\varepsilon = 0.478$ . Here the measure of the points that are attracted to the synchronized chaotic state becomes very small, and the majority of initial conditions lead to diverging orbits.

Figure 8 shows a scan of the transverse Lyapunov exponent  $\lambda_{\perp}$  for  $a = a_1$  where the individual map  $f_a$  exhibits a two-band chaotic attractor. Inspection of the figure shows that we now have two regions of weak stability for the synchronized chaotic state, one for positive values and one for negative values of  $\varepsilon$ . In the region of negative coupling constants, blowout bifurcations occur at  $\varepsilon \cong -1.472$  and  $\varepsilon \cong -1.0385$ . The region of absolute stability extends from  $\varepsilon \cong -1.464$  to  $\varepsilon \cong -1.156$ . At both ends of this region, the in-phase period-2 cycle becomes transversally unstable.

Figures 9(a)–9(c) show typical examples of the basins of attraction observed in this region. At the same time, they illustrate an interesting change in the chaotic dynamics. In Fig. 9(a) ( $\varepsilon = -1.3$ ) we have an absolutely stable two-band attractor  $A_1$  on the main diagonal. There are holes in the basin of attraction. However, these holes do not emanate from points embedded in the attractor. Hence the basin is not riddled, but has a fractal boundary.

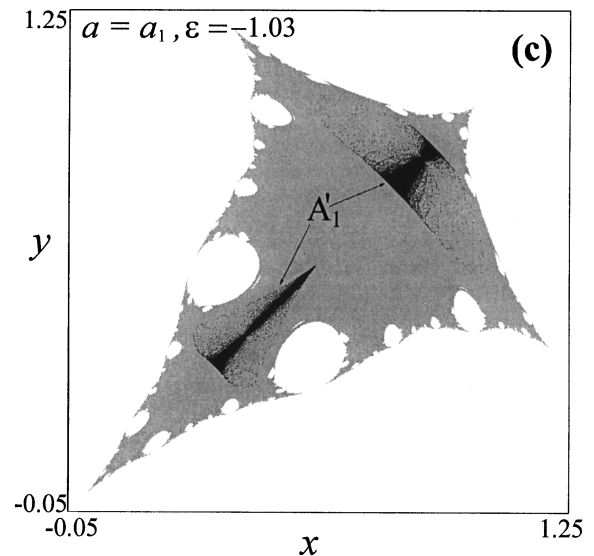
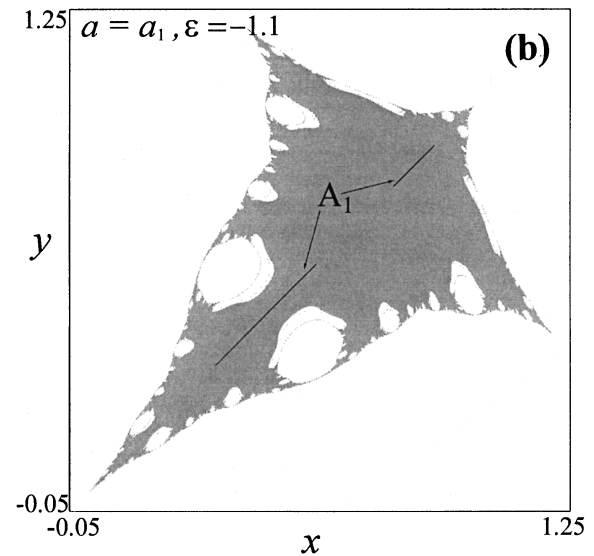
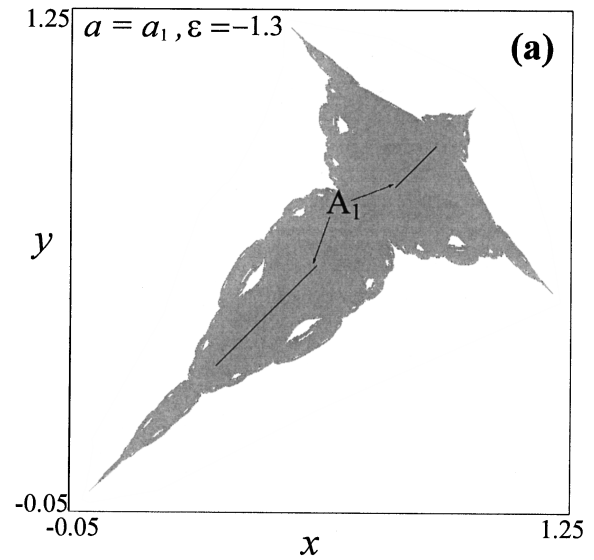


FIG. 9. Basins of attraction for different values of the coupling parameter for  $a = a_1$ : (a) fractal basin boundary for absolutely stable attractor, (b) locally riddled basin for weakly stable attractor, and (c) two-dimensional attractor restricted to the absorbing area.



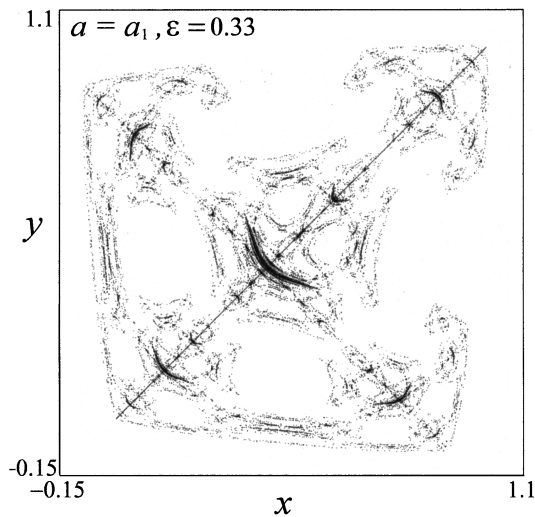


FIG. 10. Basin of attraction for  $a = a_1$  and  $\epsilon = 0.33$ .

Figure 9(b) was obtained for  $\epsilon = -1.1$ , i.e., immediately after the loss of global stability in the riddling bifurcation at  $\epsilon \cong -1.156$ . This provides a new example of a locally riddled basin. Trajectories that are repelled from the main diagonal do not reach the basin boundary, but sooner or later return to the neighborhood of the synchronized state. As  $\epsilon$  is increased slightly more, we observe a spontaneous breaking of the symmetry as the chaotic attractor spreads into two-dimensional phase space. The basin of attraction, on the other hand, only changes a little. This is shown in Fig. 9(c) for  $\epsilon = -1.03$ . The two-dimensional attractor  $A'_1$  is bounded in phase space to an absorbing area defined by the iterates of the critical curves for  $F_{a,\epsilon}$  [21,28]. The absorbing area lies fully within the basin of attraction, and as long as there is no contact between the two boundaries, the two-dimensional attractor continues to exist. With further increase of  $\epsilon$  (approximately at  $\epsilon = -0.95$ ) a crisis takes place in which the borderline of the absorbing area touches the basin boundary, and the two-dimensional attractor suddenly disappears.

Figure 10 shows an example of the basins of attraction one can observe in the other parameter window of weak stability for  $a = a_1$ . Here  $\epsilon = 0.33$ .

For  $a = a_2$ , a scan of the transverse Lyapunov exponent shows four (partly overlapping) regions of weak stability. This is illustrated in Fig. 11. The largest region extends from

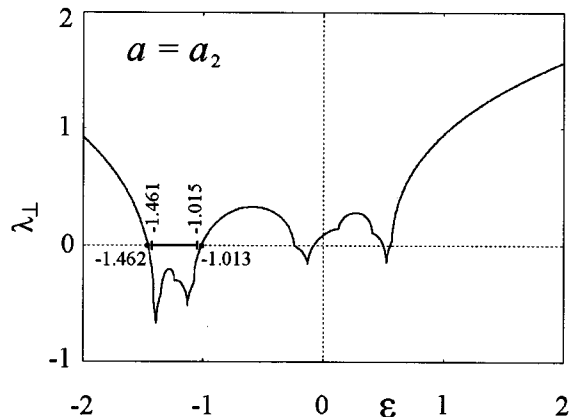


FIG. 11. Variation of the transverse Lyapunov exponent  $\lambda_{\perp}$  with the coupling parameter  $\epsilon$  for  $a = a_2$ .

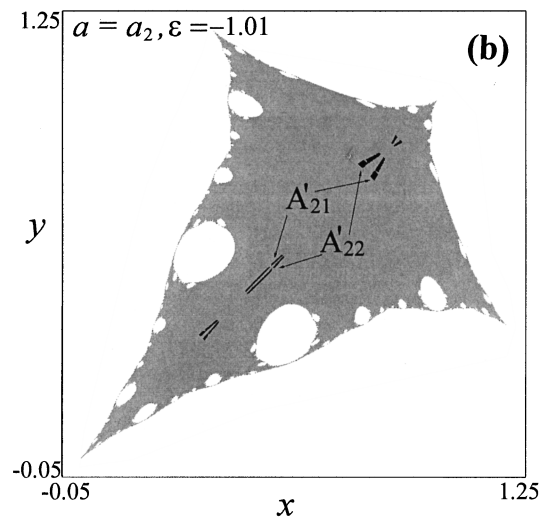
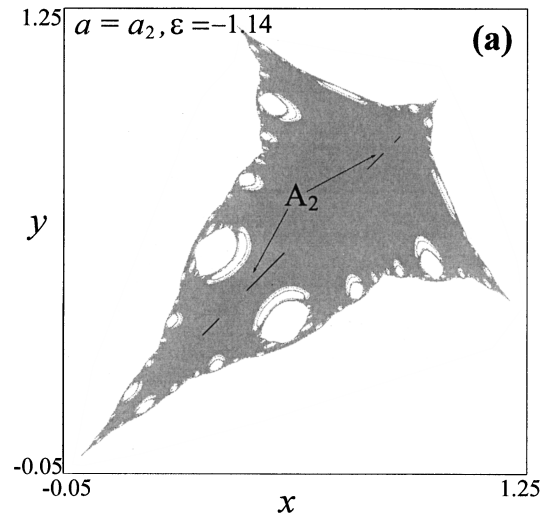


FIG. 12. Basins of attraction for  $a = a_2$ : (a) locally riddled basin with fractal basin boundary, and (b) two coexisting eight-band chaotic attractors.

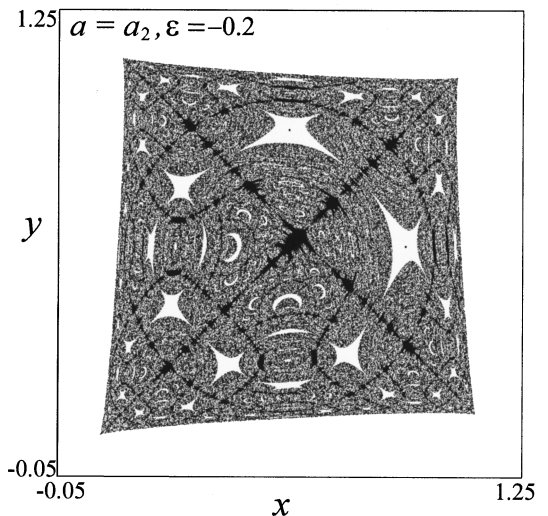


FIG. 13. The basin of attraction for the synchronous chaotic state is riddled with holes that belong to the basin of a coexisting periodic cycle.

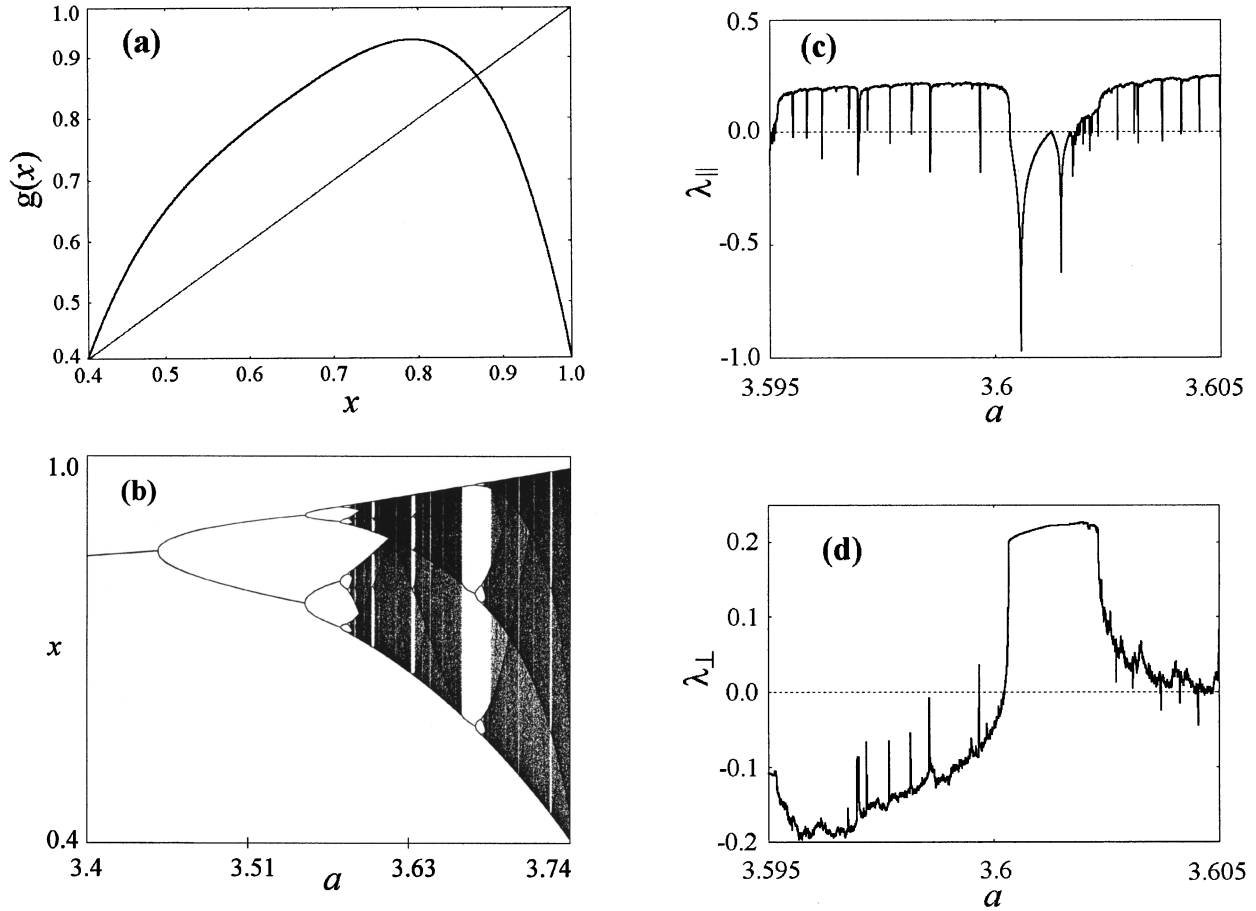


FIG. 14. Chaotic attractors off the main diagonal: (a) sketch of the one-dimensional map  $g(x)$ , (b) its bifurcation diagram, (c) the corresponding longitudinal Lyapunov exponent, and (d) the transversal Lyapunov exponent.

the blowout bifurcation at  $\varepsilon \cong -1.462$  to the blowout bifurcation at  $\varepsilon \cong -1.0134$ . Within this region we find a region of strong stability delineated by the riddling bifurcations at  $\varepsilon \cong -1.461$  and  $\varepsilon \cong -1.015$ . In both of these bifurcations, the in-phase period-8 cycle becomes transversely unstable.

Figure 12(a) shows the locally riddled basin of attraction with fractal boundaries that one can observe for  $\varepsilon = -1.14$ . In Fig. 12(b) the coupling parameter is increased to  $\varepsilon = -1.0132$ . This is immediately after the blowout bifurcation. The basin of attraction remains practically unaffected by this change. However, the dynamics of the coupled map system spontaneously breaks the symmetry, and the synchronized four-band attractor is replaced by two mutually symmetric two-dimensional eight-band attractors.

Finally, Fig. 13 shows the basin of attraction for the synchronized four-band attractor in the second parameter window of weak stability ( $a = a_2$ ,  $\varepsilon = -0.2$ ). For these parameter values the synchronized chaotic state coexists with a stable period-2 point cycle, and the basin of attraction for the chaotic state is riddled with holes that belong to the basin of attraction of the point cycle.

## V. INTERMINGLED BASINS OF ATTRACTION

Consider the map  $F_{a,\varepsilon}$  for  $\varepsilon = -1$ :

$$F_{-1} : \begin{Bmatrix} x \\ y \end{Bmatrix} \rightarrow \begin{Bmatrix} ax(1-x) - (y-x) \\ ay(1-y) - (x-y) \end{Bmatrix}. \quad (12)$$

It is easy to show that for any  $a$  the two mutually perpendicular straight lines  $x = x_2$  and  $y = x_2$  both remain invariant under two iterations of  $F_{-1}$ , i.e.,  $F_{-1}^2(\{x = x_2\}) \subset \{x = x_2\}$  and  $F_{-1}^2(\{y = x_2\}) \subset \{y = x_2\}$ . Here  $x_2$ , as given by Eq. (10), is the larger of the two amplitudes  $x_{1,2}$  for the period-2 cycle  $\gamma_2$ .

Let  $g: x \rightarrow g(x)$ ,  $x \in R^1$  denote the one-dimensional map that  $F_{-1}^2$  induces along these lines, i.e.,

$$(g(x), x_2) \equiv F_{-1}^2(x, x_2). \quad (13)$$

Figure 14(a) portrays the function  $g(x)$  for  $a = 3.6$ , and Fig. 14(b) shows the bifurcation diagram obtained by varying  $a$  over the interval from 3.4 to 3.74. Figures 14(c) and 14(d) provide scans of the corresponding longitudinal and transversal Lyapunov exponents  $\lambda_{\parallel}$  and  $\lambda_{\perp}$ , respectively.  $g(x)$  has a finite interval over which it is unimodal, and Fig. 14(b) demonstrates that it produces a transition to chaos in accordance with the usual Feigenbaum scenario. Magnifications of Figs. 14(c) and 14(d) show that  $\lambda_{\parallel}$  is positive for  $a = 3.6$ , and  $\lambda_{\perp}$  is negative. Hence for this value of  $a$  the numerical calculations indicate that  $g(x)$  displays a two-band chaotic attractor.

By virtue of its symmetry with respect to the main diagonal, the map  $F_{-1}$  displays two one-dimensional four-band

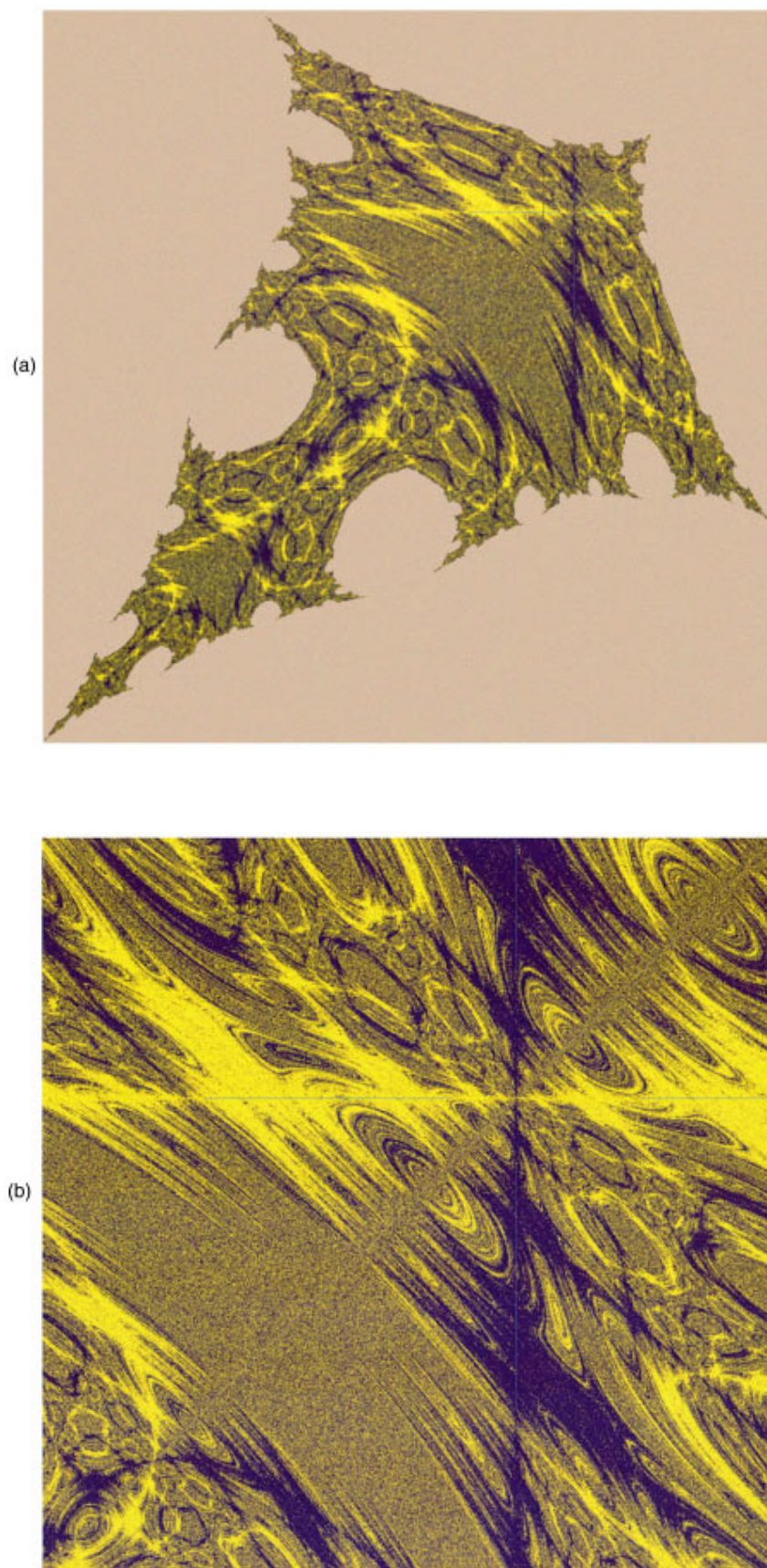


FIG. 15. (Color) Intermingled basins of attraction for two coexisting chaotic attractors: (a) overview, and (b) detail around one of the points of the period-2 cycle.

invariant chaotic sets  $A_1$  and  $A_2$ . Figure 15 displays the basins of attraction for each of these sets. For  $a=3.6$  and  $\varepsilon = -1$ , the synchronized state on the main diagonal is a chaotic saddle, and almost all trajectories that remain finite either approach  $A_1$  or  $A_2$ . However, for both of these sets the basin of attraction is riddled with holes that belong to the basin of the other set. Hence, the basins of attraction exhibit an intermingled structure with one half measure set of points that are attracted to  $A_1$ , and one half measure set that is attracted to  $A_2$ . Figure 15(b) shows a magnification of the intermingled basin structure in a region around  $(x_2, x_2)$ .

## VI. DISCUSSION

We performed a relatively detailed investigation of the formation of riddled basins of attraction for a system of two coupled logistic maps. The same phenomenon is likely to arise in almost all cases of symmetrically coupled, identical nonlinear oscillators when chaotic synchronization can be achieved. In order to determine the regions of asymptotic stability for the synchronized chaotic state, we calculated the bifurcation curves for the transverse destabilization of the main low-periodic cycles embedded in the attractor. These bifurcations are either of period-doubling type ( $\nu_2 = -1$ ) or they are pitchforks ( $\nu_2 = +1$ ). Intuitively, there are good reasons to suppose that destabilization of cycles of low periodicity plays a critical role [17,29]. For point cycles of higher periodicity, the transversal eigenvalue will presumably approach the average eigenvalue for the attractor as a whole. Since riddling arises in a region where  $\lambda_\perp < 0$ , the

average transversal eigenvalue is numerically less than unity.

Our analysis has led us to propose two different routes for the development of the basin of attraction, depending on the sequence in which an essential boundary crisis and the blow-out bifurcation occur. Related to these scenarios is an important distinction between locally and globally riddled basins. The boundary crisis is associated with the fact that we deal with noninvertible maps. Inside the basin of attraction we may then find an invariant area (the absorbing area) that is bounded by the iterates of the critical curves for  $F_{a,\varepsilon}$ . Trajectories repelled from the synchronized chaotic state are restricted by the nonlinearities of the system to move within this invariant area, and hence do not reach the basin boundary. Under these conditions the riddling is local. Variation of a parameter may cause the borderline of the absorbing area to make contact with the basin boundary, and global riddling can arise.

The existence of an invariant region bounded by the iterates of the critical curves also allows the emergence of a two-dimensional attractor. In contrast to the riddling phenomenon that depends critically on the attractor lying in an invariant subspace of total phase space, the two-dimensional attractor persists even if the symmetry is broken.

## ACKNOWLEDGMENTS

We thank T. Kapitaniak, L. Gardini, and G.-I. Bischi for a number of illuminating discussions, particularly concerning the role of the absorbing area.

- 
- [1] H. Fujisaka and T. Yamada, Prog. Theor. Phys. **69**, 32 (1983).
  - [2] A. S. Pikovsky, Z. Phys. B **55**, 149 (1984).
  - [3] L. M. Pecora and T. L. Carroll, Phys. Rev. Lett. **64**, 821 (1991).
  - [4] C. W. Wu and L. O. Chua, Int. J. Bifurcation Chaos Appl. Sci. Eng. **4**, 979 (1994).
  - [5] N. F. Rulkov, Chaos **6**, 262 (1996).
  - [6] J. C. Alexander, J. A. Yorke, Z. You, and I. Kan, Int. J. Bifurcation Chaos Appl. Sci. Eng. **2**, 795 (1992); J. C. Alexander, B. R. Hunt, I. Kan, and J. A. Yorke, Erg. Theoret. Dyn. Syst. **16**, 651 (1996).
  - [7] J. C. Sommerer and E. Ott, Nature (London) **365**, 136 (1993); E. Ott and J. C. Sommerer, Phys. Lett. A **188**, 39 (1994).
  - [8] E. Ott, J. C. Sommerer, J. C. Alexander, I. Kan, and J. A. Yorke, Phys. Rev. Lett. **71**, 4134 (1993).
  - [9] N. Platt, E. A. Spiegel, and C. Tresser, Phys. Rev. Lett. **70**, 279 (1993).
  - [10] H. Fujisaka and T. Yamada, Prog. Theor. Phys. **75**, 1087 (1986).
  - [11] L. Yu, E. Ott, and Q. Chen, Physica D **53**, 102 (1992).
  - [12] C. Grebogi, E. Ott, and J. A. Yorke, Phys. Rev. Lett. **48**, 1507 (1982); Physica D **24**, 243 (1987).
  - [13] P. Ashwin, J. Buescu, and I. Stewart, Phys. Lett. A **193**, 126 (1994).
  - [14] J. F. Heagy, T. L. Carroll, and L. M. Pecora, Phys. Rev. E **52**, R1253 (1995).
  - [15] P. Ashwin, J. Buescu, and I. Stewart, Nonlinearity **9**, 703 (1996).
  - [16] J. Milnor, Commun. Math. Phys. **99**, 177 (1985).
  - [17] Y.-C. Lai, C. Grebogi, J. A. Yorke, and S. C. Venkataramani, Phys. Rev. Lett. **77**, 55 (1996).
  - [18] Yu. L. Maistrenko, V. L. Maistrenko, A. Popovich, and E. Mosekilde (unpublished).
  - [19] Yu. Maistrenko and T. Kapitaniak, Phys. Rev. E **54**, 3285 (1996).
  - [20] A. S. Pikovsky and P. Grassberger, J. Phys. A **24**, 4587 (1991).
  - [21] L. Gardini, R. Abraham, R. J. Record, and D. Fournier-Prunaret, Int. J. Bifurcation Chaos Appl. Sci. Eng. **4**, 145 (1994).
  - [22] P. Collet and J.-P. Eckmann, *Iterated Maps of the Interval as Dynamical Systems* (Berkhauser, Boston, 1980).
  - [23] W. De Melo and S. van Strien, *One-Dimensional Dynamics* (Springer, New York, 1993).
  - [24] J. Graczyk and G. Świątek, Ann. Math. (to be published).
  - [25] M. V. Jacobson, Commun. Math. Phys. **81**, 39 (1981).
  - [26] J. Frøyland, *Introduction to Chaos and Coherence* (Institute of Physics, Bristol, 1992).
  - [27] H. E. Nusse and J. A. Yorke, Erg. Theoret. Dyn. Syst. **11**, 189 (1991).
  - [28] C. Mira, L. Gardini, A. Barngola, and J.-C. Cathala, *Chaotic Dynamics in Two-Dimensional Noninvertible Maps* (World Scientific, Singapore, 1996).
  - [29] B. R. Hunt and E. Ott, Phys. Rev. Lett. **76**, 2254 (1996).